Research Article

J Innate Immun 2025;17:522–538 DOI: 10.1159/000548548 Received: August 2, 2025 Accepted: September 15, 2025 Published online: October 31, 2025

Compartment-Specific NK Cell Phenotypes Reveal Distinct Maturation and Activation States in Inflammatory Arthritis

Franca Sophie Deicher^{a, b} Tarik Exner^c Maren Claus^d
Schayan Yousefian^{e, f, g} Lea Rodon^c Sophie Elisabeth Leonhardt^c
Jörg H.W. Distler^{a, b} Carsten Watzl^d Hanns-Martin Lorenz^c
Simon Haas^{e, f, g, h, i} Daniel Hübschmann^{j, k, l, m, n, o} Wolfgang Merkt^{a, b, c}

^aDepartment of Rheumatology, University Hospital Düsseldorf, Medical Faculty of Heinrich-Heine-University, Dusseldorf, Germany; bHiller Research Center, University Hospital Düsseldorf, Medical Faculty of Heinrich-Heine-University, Dusseldorf, Germany; Division of Rheumatology, Department of Medicine V, Heidelberg University Hospital, Heidelberg, Germany; dLeibniz Research Center for Working Environment and Human Factors at TU Dortmund (IfADo), Dortmund, Germany; eBerlin Institute of Health (BIH) at Charité Universitätsmedizin Berlin, Berlin, Germany; fBerlin Institute for Medical Systems Biology, Max Delbrück Center for Molecular Medicine in the Helmholtz Association, Berlin, Germany; ⁹Department of Hematology, Oncology and Tumor Immunology, Charité – Universitätsmedizin Berlin, Corporate Member of Freie Universität Berlin and Humboldt-Universität zu Berlin, Berlin, Germany; hPrecision Healthcare University Research Institute, Queen Mary University of London, London, UK; ⁱGerman Cancer Consortium (DKTK), Partner Site Berlin, Berlin, Germany; Innovation and Service Unit for Bioinformatics and Precision Medicine, DKFZ, Heidelberg, Germany; kComputational Oncology Group, Molecular Precision Oncology Program, NCT Heidelberg and DKFZ, Heidelberg, Germany; ^INational Center for Tumor Diseases (NCT), NCT Heidelberg, a partnership between DKFZ and Heidelberg University Hospital, Heidelberg, Germany; mPattern Recognition and Digital Medicine Group, Heidelberg Institute for Stem Cell Technology and Experimental Medicine, Heidelberg, Germany; "Institute of Human Genetics, Heidelberg University, Heidelberg, Germany; OGerman Cancer Consortium (DKTK), Core Center Heidelberg, Heidelberg, Germany

Keywords

Natural killer cells · Synovial fluid · Inflammatory arthritis · Rheumatoid arthritis · Rheumatology · Spectral flow cytometry · Proteomics

Abstract

Introduction: Synovial natural killer (NK) cells contribute to inflammation in arthritis by secreting cytokines and modulating synovial fibroblast activation. The aim of this study was

to describe systemic versus local inflammatory changes of NK cell subsets as well as their physical cell-cell interactions in arthritis patients. *Methods:* Spectral flow cytometry was used to compare paired peripheral blood (PB) and synovial fluid (SF) immune cells from patients with active inflammatory arthritis and healthy controls. Physical cell-cell interactions within

Franca Sophie Deicher and Tarik Exner contributed equally to this paper.

karger@karger.com www.karger.com/jin



© 2025 The Author(s). Published by S. Karger AG, Basel tissues were studied by applying a recently developed cellular interaction mapping framework. Results: Our paired approach revealed significant local enrichment of immature and activated NK cells in SF, characterized by elevated markers of early differentiation, immune-checkpoint regulation, and tissueresidency, highlighting tightly controlled immune activation at inflamed sites. Single-cell analysis confirmed heterogeneity within SF-NK cells, suggesting multiple co-existing activation states and developmental stages. PB-NK cells from patients differed profoundly compared to healthy controls, showing less immature NK cell subsets and an enrichment of mature, pro-inflammatory subsets indicative of systemic immune activation. Cellular interaction mapping revealed mainly NK/ neutrophil interactions of patients' NK cells, while interactions with B-cells, T-cells, or monocytes were negligible. T-cells also displayed profound local and systemic alterations. Cellular interaction mapping revealed that next to NK/neutrophil interactions, interactions between B-cells with monocytes and T-cells with neutrophils characterize joint inflammation. **Conclusion:** This paired high-dimensional analysis revealed systemic and local alterations in NK cell subsets shaped by coexisting developmental stages and immune regulatory mechanisms. Cellular interaction mapping indicated that neutrophils are a main interaction-partner of NK cells in inflamed joints. © 2025 The Author(s).

Published by S. Karger AG, Basel

Introduction

Natural killer (NK) cells represent an important component of the innate immune system in tissues and peripheral blood (PB; 5-20% of lymphocytes [1]). NK cells are known primarily for their cytotoxic functions against virus-infected and malignant cells, as well as their ability to regulate adaptive immune responses through cytokine production [2]. These cells are broadly divided into two major subsets: the CD56^{dim}CD16^{bright} subset, known for potent cytotoxicity, and the CD56brightCD16dim/negative subset, characterized by cytokine secretion and immunomodulatory functions [3, 4]. This functional diversity enables NK cells to play both protective and potentially pathogenic roles in chronic inflammatory diseases. However, there are substantial knowledge gaps regarding the role of NK cells in human non-infectious inflammatory diseases such as inflammatory arthritis (IA).

IA encompasses a spectrum of autoimmune and autoinflammatory disorders characterized by joint inflammation leading to tissue damage and disability. A common feature in these disorders is the accumulation of various immune cells in the synovial fluid (SF), which

drives local inflammation and joint destruction [5]. Although T-cells and macrophages have been traditionally emphasized in arthritis pathogenesis, increasing evidence suggests that innate lymphocytes, particularly NK cells, contribute to both systemic inflammation and localized inflammatory responses in affected joints [6].

NK cells infiltrate inflamed joints and undergo phenotypic and functional shifts influenced by the local inflammatory environment [6-8]. An increase in activated synovial NK cells with high regulatory potential has been reported [6–8]. IFNy-producing NK cells were associated with erosions in rheumatoid arthritis (RA) [7]. We recently showed that NK cells interact with synovial fibroblasts [8]. NK cells contribute to the development of a highly inflammatory subtype in synovial fibroblasts, characterized by MHC-II-expression, antigen-presentation, and IL-6 production [8, 9]. Conventional flow cytometry analyses in RA showed that SF-NK cells belong to the CD56^{bright} phenotype, marked by elevated expression of activation markers such as CD69 and reduced cytotoxic potential compared to PB NK cells [3, 6, 10]. In psoriatic and other arthritides, similar alterations of SF-NK cells have been reported, indicating a tailored local adaptation as a general feature in synovial inflammation [11].

Notably, substantial knowledge gaps and controversies remain regarding the developmental origin, functional plasticity, and precise contributions of NK cells to arthritis pathogenesis. One prominent debate centres around the identity and function of immature versus mature NK cell subsets within inflamed joints. Specifically, the potential differentiation trajectory of SF-NK cells remains unclear [3, 6]. Lacking analysis of paired samples, the compartment effect also remains understudied precluding a direct comparison of blood vs. synovial NK cells. These questions remain unanswered to date, partly due to limitations in non-human modelling of these diseases and limited access to human tissue of patients suffering from these diseases. Importantly, comprehensive high-dimensional analyses of paired PB and SF samples from the same patients are needed but remain rare [12]. Paired blood-SF datasets have the potential to provide essential insights into systemic versus localized immune activation and -regulation. Moreover, such datasets allow description of localization- and disease-specific NK cell changes that are not secondary to treatments, as the comparator (PB) is equally exposed to those treatments. These paired analyses are therefore crucial to delineate the relationship between peripheral immune dysfunction and jointspecific inflammatory responses, offering potential

therapeutic targets tailored to specific activation states or lymphocyte subsets [5, 7].

Our investigation described here aimed to elucidate common systemic versus local NK cell alterations, focusing particularly on developmental stages, activation states, and immune regulatory mechanisms operative in inflamed joints. We performed detailed spectral flow cytometry analyses of paired PB and SF samples from patients with active IA, including diverse disease entities, and compared these profiles with healthy controls. In addition, we leverage interact-omics [13], a recently published innovative interaction mapping framework that analyses cell doublets as surrogate parameters for cell-cell interactions. We use this framework to delineate cell-cell interactions in inflamed joints compared to PB and healthy controls. Further, we use an innovative approach of developmental trajectory mapping to determine the maturity and activation status of SF-NK cells. This paired, comprehensive approach allows insights into compartment-specific alterations of NK cells in joint inflammation.

Material and Methods

Patients and Materials

Informed written consent was obtained from all donors of PB and SF. Clinical data were gathered from patient records, and the local institutional review board approved this study (University of Heidelberg, S-272/2021). Data and samples were pseudonymized. Patient and healthy donor characteristics are detailed in Table 1.

Sample Asservation and Preparation

PB mononuclear cells (PBMCs) were isolated from heparinized blood from healthy volunteers using density gradient centrifugation with Pancoll separating solution (Pan Biotech) and frozen immediately after isolation in Kryosafe (c.c.pro) or FCS (foetal calf serum) + 10% dimethyl sulfoxide (DMSO). PB whole leukocytes from IA patients were prepared by ACK lysis at RT for 5 min, followed by a centrifugation at 300 g for 5 min. The supernatant was removed and the pellet was resuspended in ACK and lysed for 5 min at 4°C. The lysate was centrifuged again at 300 g for 5 min and the cells were finally frozen in Kryosafe medium. SF from IA patients with highly active arthritis was taken from diagnostic or therapeutic punctures after written informed consent. The SF was aspirated into syringes, subsequently diluted 1:10 in phosphate buffer

solution and centrifuged for 10 min at RT at 300 g. The cell pellet was resuspended in Kryosafe and frozen immediately.

Spectral Flow Cytometry Analysis

Immediately before staining, cells were slowly thawed and counted. A total of 500.000 cells were washed and stained with Zombie NIR and the staining master mix containing all antibodies, True-Stain Monocyte Blocker (Biolegend) and Brilliant Stain Buffer (BD Biosciences). After 30 min at 4°C, cells were washed again and resuspended in phosphate buffer solution with 2% human serum. For flow cytometry analysis, the BD Cytek Aurora Spectral cytometer was used. Quality control was performed according to the manufacturer's instructions daily before measuring.

Preprocessing and Gating of Flow Cytometry Data

Raw.fcs files were exported from the CyTEK Aurora cytometer with concurrent normalization and demultiplexing according to the manufacturer's instructions. The demultiplexed files were gated using FlowJo (BD Biosciences, v. 10.9.0) and read using FlowIO (v. 1.1.1). The gating strategy is illustrated in online supplementary Figure S1A (for all online suppl. material, see https://doi.org/10.1159/000548548). The individual files were concatenated into an AnnData (v. 0.10.2) [14] object in Python (v. 3.10.9). Firstly, the data were arcsinh-transformed using manually assigned cofactors that separate the marker-positive from marker-negative events. To gate CD45+ cells, the transformed data were clustered using the Leiden algorithm (v. 0.10.1) [15] and projected in uniform manifold approximation and projection (UMAP; v. 0.5.0) [16] space. The clusters with expression of lineage-defining markers were selected and classified as the respective cell type. NK cells were defined as cells belonging to clusters with an expression of CD45, CD16, and CD56. Monocytes were classified by the expression of CD45 and CD14. The expression of the T-cell receptor CD3 identified T-cells, while these cells grouped were further into CD8+T-cells CD4+T-cells (online suppl. Fig. S1B–D).

Diffusion Map and Differentiation Rank Analysis

Diffusion maps were calculated using the ScanPy implementation [17–19]. Firstly, 20 principal components and the resulting neighbourhood graph were calculated as described in the dimensionality reduction paragraph. For diffusion maps, 15 components were calculated. Differentiation ranks were determined using a two-step computational approach. Initially, the

Table 1. Patient cohort

Donor	Material	Sex	Age, years	Diagnosis	Immunosuppressive treatment	Disease duration	Serology	Cells/ nL SF
P1	SF, PBWL	F	36	JIA	Adalimumab 40 mg s.c./14d, sulfasalazine 1,500 mg/d, prednisolone 10 mg/d	17 years	HLA-B27+, ANA 1: 5,120	4.5
P2	SF PBWL	F	78	RA	Prednisolone 10 mg/d	N/A	RF+ (100 IU/mL), ACPA+ (340 IU/ mL), ANA neg	23.25
Р3	SF, PBWL	М	67	Gout	None	2 weeks	CRP 370 mg/L	N/A
P4	SF, PBWL	М	73	PMR	Leflunomide 20 mg/d, prednisolone 4 mg/d	17 years	RF neg., ANA neg	1.25
P5	SF, PBWL	М	49	PSA	Prednisolone 50 mg/d	11 years	RF neg., ACPA neg., CRP 223 mg/L	5.8
P6	SF, PBWL	F	46	iraE (breast cancer) DD PsA	Abemaciclib 300 mg/d	1 month	N/A	16.15
P7	SF, PBWL	F	50	RA (erosive)	Upadacitinib 15 mg/d, leflunomide 15 mg/d, methylprednisolone 8 mg/d	28 years	RF neg., ACPA neg., ANA 1:320	14.0
HD1	PBMC	F	23	-	-	-	-	-
HD2	PBMC	F	24	-	-	-	-	-
HD3	PBMC	F	20	_	-	-	-	-
HD4	PBMC	F	20	_	-	-	-	
HD5	PBMC	F	23	_	-		-	-
HD6	PBMC	F	33	_	-	-		
HD7	PBMC	F	24	_	-	-	-	-
HD8	PBMC	F	20	_	-	-	_	_
HD9	PBMC	F	22	-	-	_	-	-

P, patient; HD, healthy donor; SF, synovial fluid; PBWL, peripheral blood whole leukocytes; PBMC, peripheral blood mononuclear cells; F, female; M, male; JIA, juvenile idiopathic arthritis; RA, rheumatoid arthritis; PMR, polymyalgia rheumatica; PSA, psoriatic arthritis; Ca, carcinoma; DD, differential diagnosis; CTD, connective tissue disease; ILD, interstitial lung disease; s.c., subcutaneous; /d, per day; N/A, not available; ANA, antinuclear antibody; RF, rheumatoid factor; ACPA, anti-citrullinated protein antibody; CRP, C-reactive protein; SSA/SSB, antibodies against SS-A/SS-B.

expression levels of markers CD16, CD56, and CD57 within each cell were standardized. These markers were weighted (CD56: –1.0, CD16: 0.5, CD57: 1.0) to compute a rank score, which was then normalized to a (0, 1) range. Subsequently, we assigned differentiation rank values to all cells in the dataset by averaging the differentiation rank of their nearest healthy control neighbours. This process began by considering the five closest neighbours and expanded up to fifty neighbours if sufficient control cells were not initially found. For full implementation details, refer to the source code.

Interact-Omics Analysis

The analysis of physically interacting cells was performed according to the guidelines outlined in Vonficht et al. [13]. Initially, raw.fcs files were preprocessed using PeacoQC [20] to remove artefact events and anomalies. Populations of interest (live cells) were exported using channel values as.csv files. Further analyses were performed in R (v. 4.3.0) using the PICtR package (https://github.com/agSHaas/PICtR). In brief, the *sketch_wrapper* function was used for the classification of cells according to their FSCarea to FSC-height ratio, for downsampling using the

atomic sketching approach [21], dimensionality reduction using principal component analysis and clustering with the Louvain algorithm [22]. Finally, the data were visualized using a UMAP embedding [16]. Clusters were manually annotated using established marker expression profiles and expert curation. Clusters with interacting cells were selected and clustered using the Leiden algorithm [15] and re-annotated as described above. Clusters with more than two interacting partners were excluded from the display item but not from the calculations. For cells not included in the initial sketching, cluster identities were assigned using Linear Discriminant Analysis as implemented in the MASS R package.

Statistical Analysis

The boxplots display the median and the 25th/75th percentile (box), while the whiskers extend from minimum to maximum values (0–100%). Statistics were calculated as a pairwise the Kruskal-Wallis test, applied to two independent conditions at a time, as implemented in SciPy. For two groups, this test is mathematically the same as the Wilcoxon rank-sum (Mann-Whitney U) test and yields identical two-sided p values when the same tie correction is used; we, therefore, report these results as Wilcoxon where helpful. Comparisons with p values exceeding 0.05 have been considered non-significant.

Results

In order to delineate the phenotypes of NK cells in IA, we isolated leukocytes from PB and paired SF samples from 7 patients with active IA of different disease entities. As a control for the phenotypes of circulating mononuclear cells, PBMCs of nine healthy donors were amended to the dataset (Fig. 1a; Table 1). We used spectral flow cytometry with a panel of 28 markers, covering markers for viability, cell type identification, activation, and ontogeny (online suppl. Fig. S1; Table 2). NK cells, CD8+T-cells, CD4+T-cells, and monocytes were all detectable in all SF samples, and there were no significant changes in the relative frequency of these cells among gated mononuclear cells in PB of patients with IA compared to healthy controls (Fig. 1b). NK cell frequencies were slightly lower in inflamed SF compared to PB (Fig. 1b).

NK Cells Display Compartment- and Arthritis-Associated Phenotypes in IA

Hierarchical clustering and principal component analysis of NK cells based on the marker expression on a pseudo-bulk-level revealed a clear phenotypic separation of SF-NK cells compared to paired PB-NK cells of the same patients (Fig. 1c, d). Interestingly, PB-NK cells from patients were phenotypically distinct from healthy controls (Fig. 1c, d). In PB, patient NK cells exhibited a significantly increased expression of CD161, KLRG1, TIGIT, and 41BB as well as a decreased expression of CTLA4, CD56, CD38, and PD-1 as compared to healthy controls (Fig. 1e). In contrast, SF-NK cells were characterized by a significantly increased expression of NKG2A, CD56, CTLA4, CD69, 41BB, and HLA-DR and an accompanied downregulation of CD16 and CD57 compared to paired PB-NK cells from the same patients (Fig. 1e). Per-sample analysis of protein expression levels on NK cells comparing all three groups is shown in online supplementary Figure S2.

Phenotypic Heterogeneity of NK Cells in PB and SF in IA

Projection of single NK cells into UMAP-space suggested a clear distinction of NK cells originating from PB and SF of patients with IA (Fig. 2a). SF-NK cells were characterized by a higher expression of CD56, CD69, and NKG2A with a notably lower expression of CD16 and CD57 when compared to PB-NK cells of both healthy donors and patients (Fig. 2b, n = 7 IA patients, n = 9 healthy controls). We noticed visually discernible subtypes within SF-NK cells. These subtypes were characterized by a differential CD56 and CD16 as well as CD69 expression, the latter of which was unique to, but did not cover all SF-NK cells (Fig. 2b). To confirm these NK cell-subsets in SF, we used unsupervised Leiden clustering on exclusively SF-NK cells. Leiden clustering identified a total of seven clusters of SF-NK cells which were subsequently merged into three metaclusters (Fig. 2c). These metaclusters were characterized by differential expression of NKG2A, CD16, CD56, CD69, CD57, and CTLA4, likely representing different activation states or maturation stages of SF-NK cells (Fig. 2d, e, online suppl. Fig. S3).

Maturation Analysis Suggests the Presence of less Differentiated NK Cells in SF

Several differentially expressed surface markers on SF-NK cell metaclusters (including CD16, CD56, and CD69) are recognized markers for NK cell activation, tissue-residency, maturation, and ontogeny at the same time, depending on the experimental condition. This limits the interpretation of earlier studies suggesting the presence of immature NK cells in inflamed joints and requires alternative approaches for confirmation. In order to overcome, these limitations and to alternatively delineate the

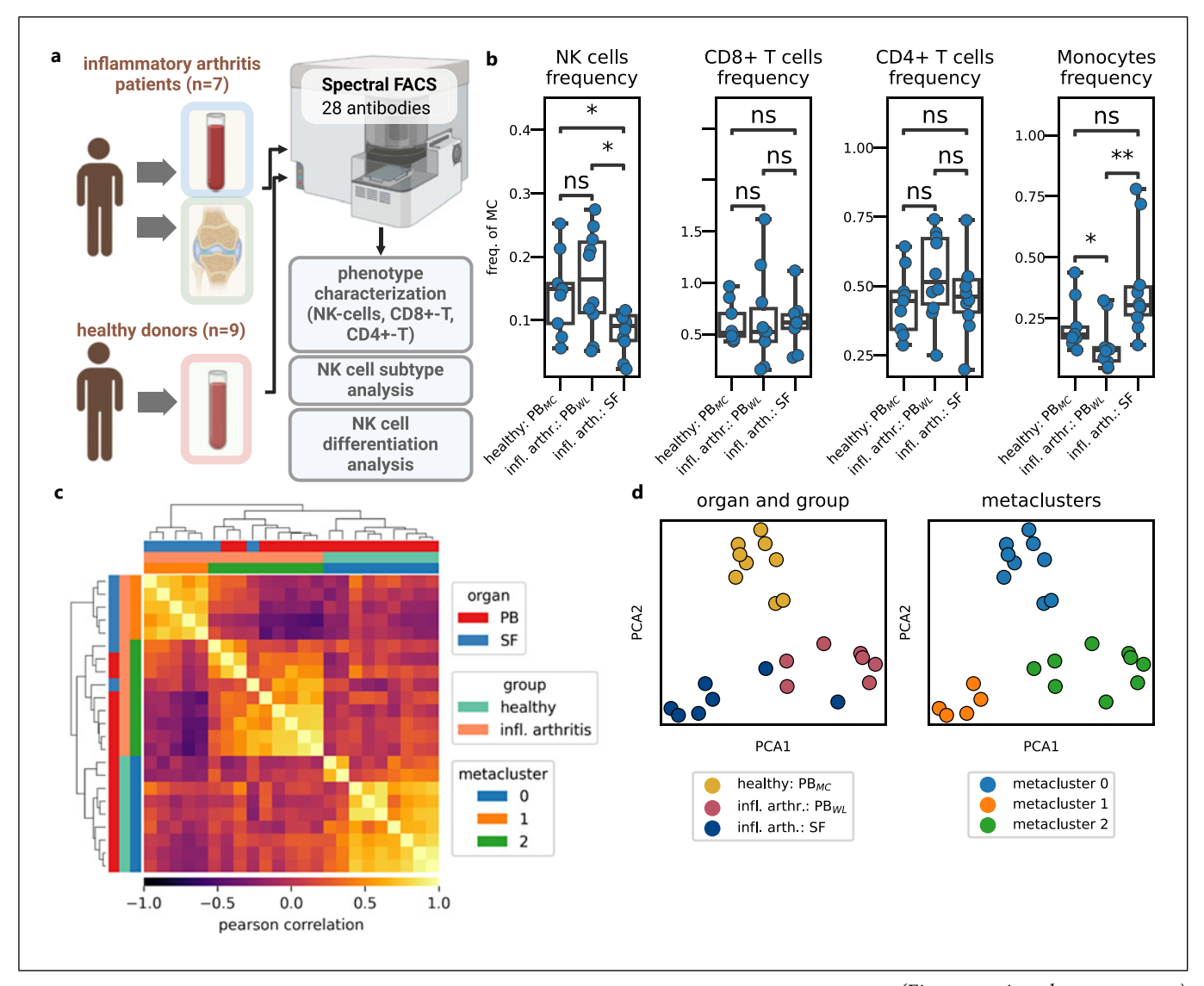


(Figure continued on next page.)

developmental stages of NK cell subsets in arthritis patients, we calculated a proportional differentiation rank of PB-NK cells of healthy donors (n=9) using the weighted expression of CD56, CD16, and CD57. We then mapped patient NK cells (n=7) onto this differentiation spectrum and visualized them in a combined diffusion map embedding [19] to visualize the differentiation trajectory on NK cells on our dataset (Fig. 3a; online suppl. Fig. S4 and Methods). In SF, we observed an enrichment of NK cells of which the cell surface proteome was similar to the potentially earliest maturation stages found in PB in healthy controls (Fig. 3b). In parallel, the frequency of CD57^{bright} cells was reduced in PB of IA patients, confirming an accumulation of potentially immature NK cells in SF

(Fig. 3b). These immature cells were associated with a lower expression of CD161, KLRG1, CD45, and TIGIT as well as a higher expression of CD27, NKG2A, and CTLA4 across compartments (online suppl. Fig. S5). We confirmed the analysis by excluding the three markers CD16, CD56, and CD57 in the mapping (not shown), thus confirming the immaturity of SF-NK cells independent of these markers.

Differential Phenotypes of CD8+- and CD4+T-Cells in IA

Following our approach as described above, we found clear shifts in the marker profile of both cytotoxic (CD8+) and helper (CD4+) T-cells in

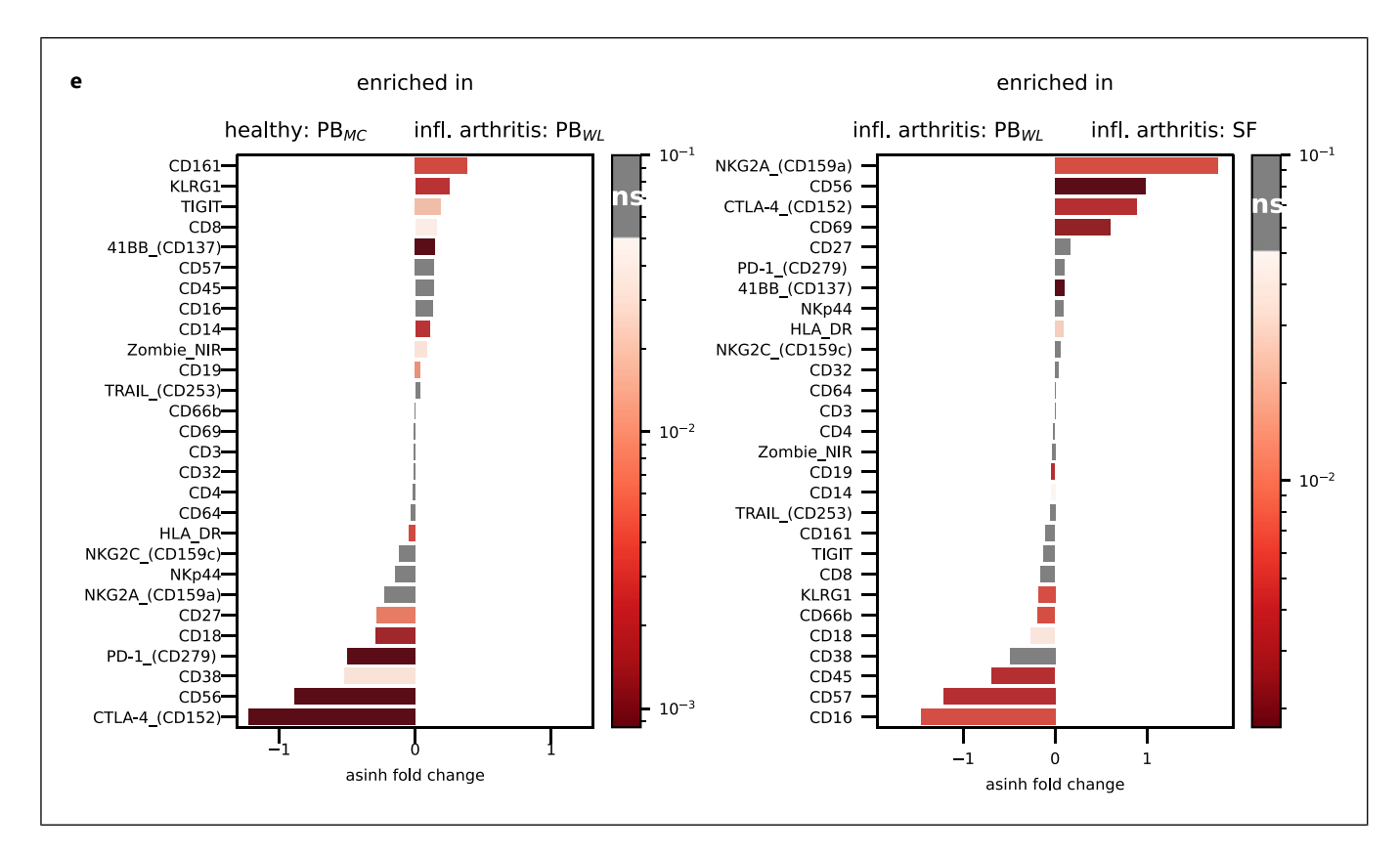


Fig. 1. NK cells display phenotypic changes in PB and synovial fluid in patients with inflammatory arthritis. **a** Graphical experimental design. Of note, from patients, only paired blood and synovial fluid samples were used in this study. **b** Cell frequencies. Frequencies of the indicated cell types were plotted as a percentage of mononuclear cells. Wilcoxon test was used to compute statistical significance. p > 0.05: n.s., p < 0.05: *, p < 0.01: ***c Sample correlation analysis on a pseudo-bulk level. NK cells were correlated as described in the (online suppl) Methods section. Hierarchical clustering revealed three subgroups which correspond to cells of different tissue and patient group (healthy and IA). **d** Sample-wise principal component analysis (PCA). Samples were grouped by PCA and coloured by tissue and patient group (left) and the metaclusters (right) as calculated in C. **e** Differential expres-

sion analysis. Fold-changes (x-axis, asinh_fc) were calculated as described in the (online suppl) Methods section. Notably, NK cells analysed from PB show significant phenotypic differences comparing healthy controls and patients with IA, including expression changes of CD161, KLRG1, PD-1 and CD56. Comparison of NK cells extracted from PB and SF show a differential phenotype with the elevation of activation markers such as NKG2A and CD69 and the corresponding downregulation of CD16 and CD57. p-values were calculated as described in the Methods section (Kruskal) where p values above 0.05 were considered not significant (n.s.). For comparison, the data are presented as boxplots in online supplementary Figure S2. Healthy controls n = 9, IA patients n = 7. PB: peripheral blood, SF, synovial fluid; IA, inflammatory arthritis.

PB from patients compared to healthy controls: Both subsets showed higher TIGIT, KLRG1, and CD16 expression together with a common decrease of CD27. Further downregulated markers in CD8+T-cells included CTLA4, NKG2A, and CD69, while CD38 was downregulated in CD4+T-cells (Fig. 4; online suppl. Fig. S6–S8, n = 7 IA patients, n = 9 healthy controls). Compared to paired PB-T-cells, SF-T-cells were characterized by further upregulation of PD-1, TIGIT, and HLA-DR in both subsets, alongside raised CD69 on CD4+ cells,

yielding several clusters that differed mainly in PD-1, CD69, HLA-DR, and TIGIT expression (Fig. 4a-e; online suppl. Fig. S6-S8).

Mapping of Physically Interacting Cells in Inflamed SF

The analyses described above indicated a unique phenotype of SF-NK cells. Under the premise that direct intercellular communications shape phenotypes and vice versa, we next wanted to elucidate which other cell types NK cells interact with in arthritis. Instead of using

Table 2. Twenty-eight-colour-antibody panel

Target	Fluorophore	Dilution	Distributor	Catalogue No.	Clone
CD38	BUV395	1:100	BD Biosciences	#563811	HB7 (RUO)
CD159c (NKG2C)	BUV496	1:50	BD Biosciences	#749844	134,591 (RUO)
CD3	BUV563	1:200	BD Biosciences	#748569	UCHT1
CD16	BUV615	1:400	BD Biosciences	#751572	3G8
CD161	BUV661	1:100	BD Biosciences	#750596	HP-3G10
CD32	BUV737	1:50	BD Biosciences	#741835	FLI8.26
CD56	BUV805	1:500	BD Biosciences	#742022	B159
CD137 (41BB)	BV421	1:50	Biolegend	#309820	4B4-1
CD4	V450	1:200	BD Biosciences	#560345	RPA-T4
CD64	BV480	1:200	BD Biosciences	#566129	10.1
KLRG1	BV510	1:50	Biolegend	#138421	2F1/KLRG1
CD45	BV570	1:400	Biolegend	#304034	HI30
HLA-DR	BV605	1:50	Biolegend	#307640	L243
CD19	BV650	1:200	Biolegend	#302238	HIB19
NKp44	BV711	1:200	BD Biosciences	#744303	p44-8
CD69	BV750	1:400	Biolegend	#310954	FN50
TIGIT	BV786	1:100	BD Biosciences	#747838	741,182
CD57	FITC	1:400	Biolegend	#359604	HNK-1
CD8	AF532	1:200	ThermoFischer Scientific	#58-0088-42	RPA-T8
CD14	BB700	1:1,000	BD Biosciences	#566465	ΜφΡ9
CD27	PerCp-Cy5.5	1:50	BD Biosciences	#560612	M-T271
CD159a (NKG2A)	PE	1:100	Beckman Coulter	#IM3291U	Z199
CD152 (CTLA4)	PE-Dazzle	1:100	Biolegend	#369616	BNI3
CD253 (TRAIL)	PE-Cy7	1:50	Biolegend	#109312	N2B2
CD279 (PD-1)	AF647	1:100	BD Biosciences	#560838	EH12.1
CD18	AF700	1:800	Biolegend	#302124	TS1/18
Zombie NIR	Zombie NIR	1:700	Biolegend	#423106	-
CD66b	APC-Fire 750	1:400	Biolegend	#396908	QA17A51

indirect bioinformatics-based analyses as known from single-cell RNA-seq-studies that rely on inference of cell-cell communication, we mapped physically interacting cells by applying the analytical interact-omics framework [13] on the spectral flow cytometry dataset (Fig. 5, n=7 IA patients, n=9 healthy controls). Interact-omics leverages multi-parameter flow cytometry to generate an unbiased map of physically interacting cells. This adds a critical layer of information that conventional single-cell approaches, which provide only static snapshots, often overlook and offers novel insights into the complex

cellular networks underlying IA. Given that cell-cell interactions may result from both biological and technical factors, we sought to limit technical influences by focusing on interactions within, rather than across compartments.

In healthy blood, we found that NK cells have the potential to interact with several cell types, even though event counts in specific subsets were low and require careful interpretation. In patient blood and SF, NK cells were found to be predominantly interacting with neutrophils (Fig. 5a). Interestingly, in SF, the

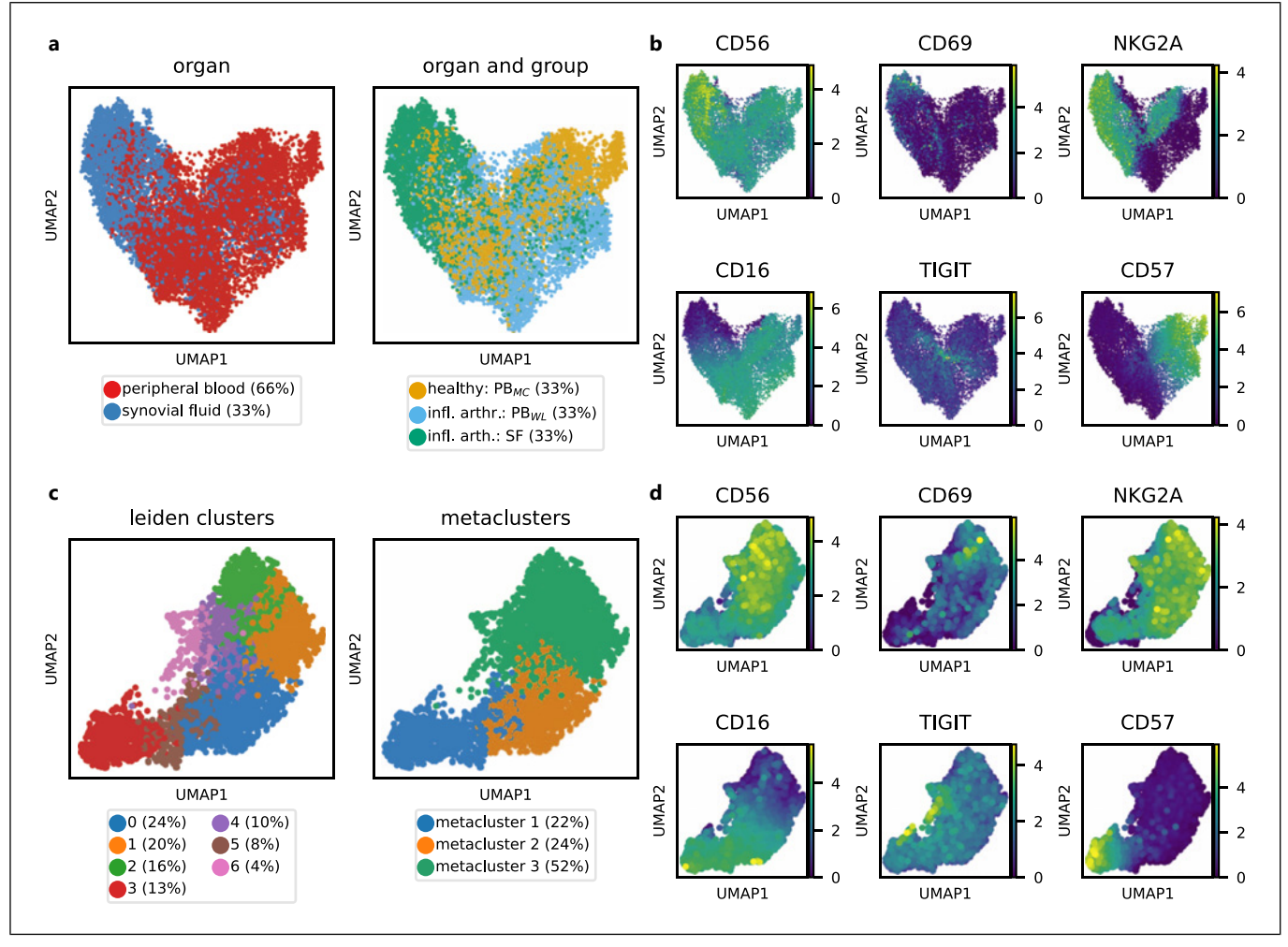


(Figure continued on next page.)

interactome was overall dominated by interactions between monocytes and B-cells, whereas in healthy blood, monocytes rather interacted with T-cells. Although our study design does not allow for a direct tissue comparison, these findings highlight how the cellular interaction landscape differs by condition (Fig. 5b).

Discussion

In this study, we analysed lymphocyte phenotypes using paired samples of PB and SF from patients with IA. Despite various underlying diseases with potentially differing mechanisms, every patient exhibited severe joint swelling combined with high cell counts in the SF, indicating a consistent clinical

phenotype of intense inflammation. Although the current data do not allow for conclusions regarding individual diseases, they show similarities and common features of IA. The differences of lymphocyte subsets in blood found in patients compared to healthy controls may be partially secondary to treatment and cell purification (see Methods), presenting a potential limitation of our study. It is in contrast a strength of our dataset that the differences within paired samples, the focus of our study, cannot be confounded by treatment.

The spectral flow cytometry panel was primarily designed to study NK cell biology, but also the most common lineage markers were included. Given overlaps of important cell surface receptors between NK cells and T-cells, we were also able to describe T-cells.

2

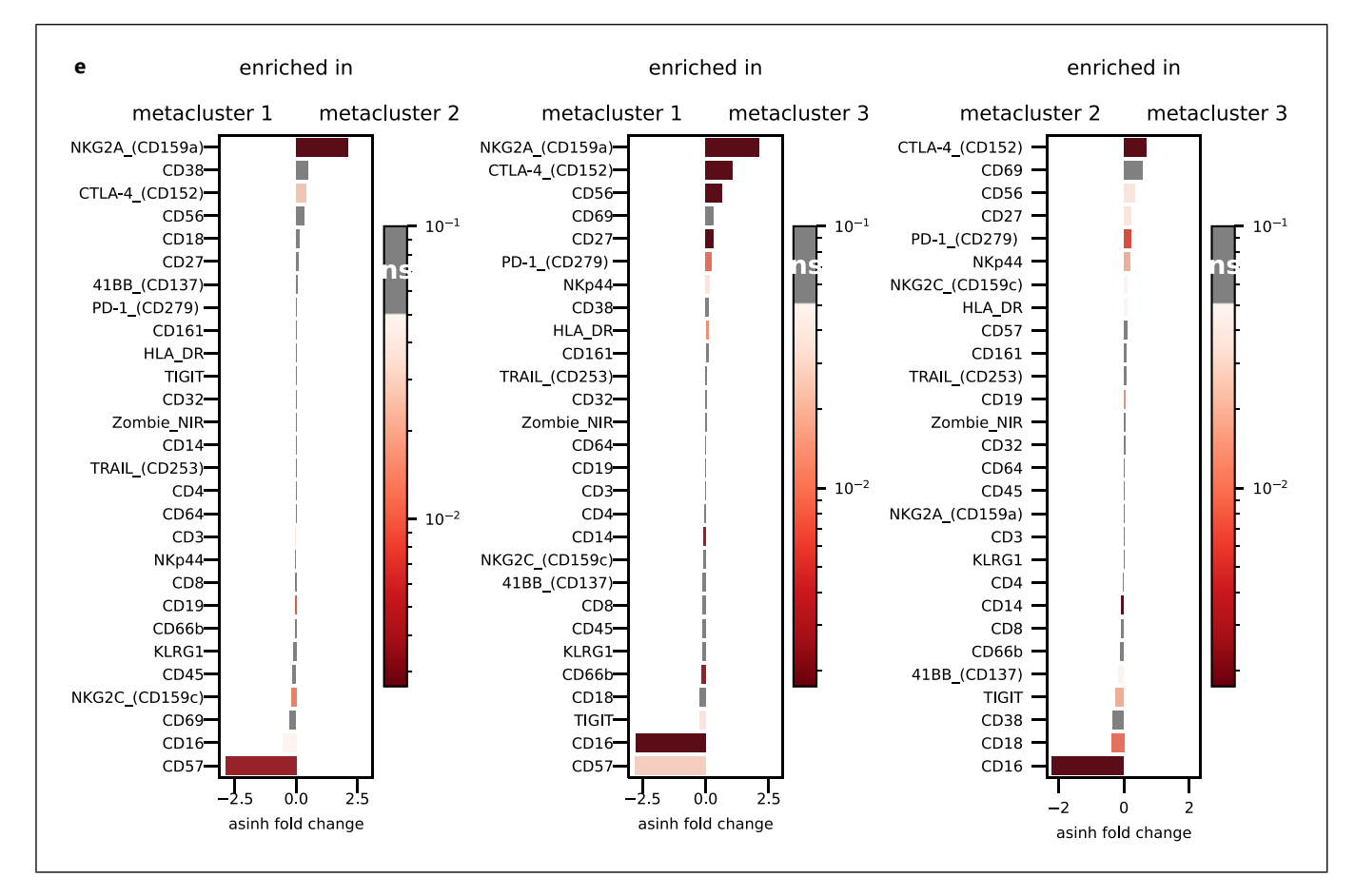


Fig. 2. Subgroups of NK cells in synovial fluid. a Left: UMAP representation of NK cells in PB and SF. Right: UMAP coloured by tissue and patient cohort. b Embedding as in A, coloured by the indicated marker proteins. Notably, a diversification of NK cells was observed in SF, characterized by the contrastive expression of CD56 and NKG2A for one subset of cells and expression of CD69 for another subset of cells. Corresponding boxplot representations are shown in online supplementary Figure S2. c UMAP embedding of SF-NK cells only. Left: coloured by Leiden clusters. Right: coloured by metacluster which were obtained by merging the Leiden

clusters. **d** Embedding as in C, coloured by the indicated marker proteins. Three subsets can be observed, which are characterized by differential expression of CD56, CD16 and CD69, together with other activation markers (e.g., TIGIT). **e** Differential expression of metaclusters as shown in C. p values were calculated as described in the Methods section (Kruskal) where p values above 0.05 were considered not significant (n.s.). For comparison, the data are presented as boxplots in online supplementary Figure S3. Healthy controls n = 9, IA patients n = 7. PB, peripheral blood; SF, synovial fluid; IA, inflammatory arthritis.

Differential T-Cell Immunophenotypes in IA: Elevated Checkpoint and Differentiation Markers in PB and SF

We noticed phenotypic changes within PB cells in patients with IA compared to healthy controls. The observed changes in CD8+T-cells and CD4+T-cells accompanied an increased expression of KLRG1, CD16, and TIGIT in IA. This suggests a more frequent abundance of terminally differentiated effector cells with signs of exhaustion in our cohort [23–27]. These cells also showed signs of inhibitory mecha-

nisms, suggesting a tightly controlled activation and suppression balance as observed for the NK cells as discussed below. The presence of these cells has been linked to various forms of inflammation in the past [27–29] and points to high burden of inflammation in the patients of our cohort. SF-CD8+T-cells and SF-CD4+T-cells were characterized by the increased expression of PD-1, TIGIT, CD69, and HLA-DR, suggesting the presence of a subset of activated, potentially exhausted CD8+- and CD4+T-cells [12, 30–33].

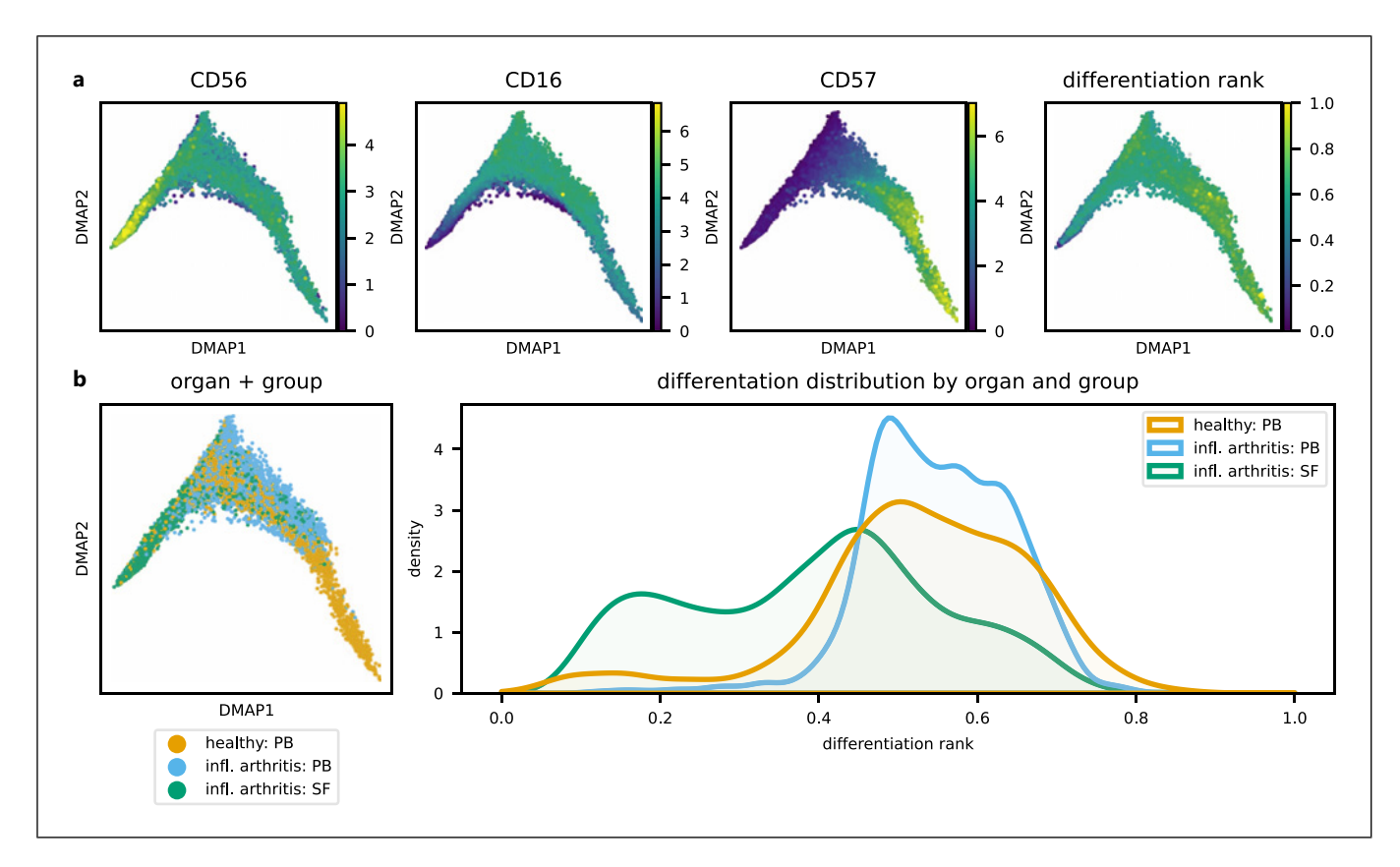


Fig. 3. Differentiation analysis of NK cells suggests the influx of immature NK cells into the inflamed synovium. **a** Diffusion Map embedding coloured by CD56, CD16 and CD57 as well as the differentiation rank along the three markers (compare Methods section). **b** Left: diffusion map embedding as in A coloured for the patient group. Right: histogram analysis shows an accumulation of less mature NK cells in the SF with concurrent reduction of these cells in PB of the same patients.

Notably, a subset of NK cells with very high differentiation rank values, characterized by a low expression of CD16 and a high expression of CD57, are present in cells from PB of healthy donors, but not in patients with IA. Marker expression across the differentiation rank has been included as online supplementary Figures S4 and S5. Healthy controls (n = 9), IA patients (n = 7). PB, peripheral blood; SF, synovial fluid; IA, inflammatory arthritis.

Phenotypic Differences of PB-NK Cells in IA

Previous studies evaluating the phenotypic differences of PB-NK cells comparing healthy donors and patients with IA are scarce and often describe distinct populations as differentially abundant [7, 10, 34–36]. Here, our high-dimensional approach allowed us to delineate striking differences of NK cells from PB comparing healthy individuals and patients with IA. Our analyses suggest that PB-NK cells in IA are characterized by a higher expression of CD161 and 41BB, indicating a proinflammatory and activated cell state [37], and a lower CD56, PD-1, and CTLA4 expression compared to NK cells from healthy controls. As CD56^{bright} NK cells are generally associated with less maturity [38], our results indicated a specific loss of immature NK cells in the PB of IA patients. This might be caused by a slower production

of NK cells, a preferential trafficking of these cells to the inflamed site, or both. The paired approach allowed us to test the hypothesis if phenotypically immature NK cells were enriched at the site of inflammation. Indeed, we confirmed the preponderance of immature NK cells in SF. Our study therefore expands previous studies [6, 7, 10, 35, 39] by showing the immaturity of SF-NK cells using the unbiased differentiation rank approach discussed in the following section.

Differentiation Rank Analysis Suggests the Presence of Immature NK Cells in the Inflamed Joint

Some of the frequently used markers of NK cell maturation and activation, especially CD56, CD16, and CD69, are contemporarily influenced by cell activation, homoeostasis, ontogeny, and tissue localization. Therefore, it

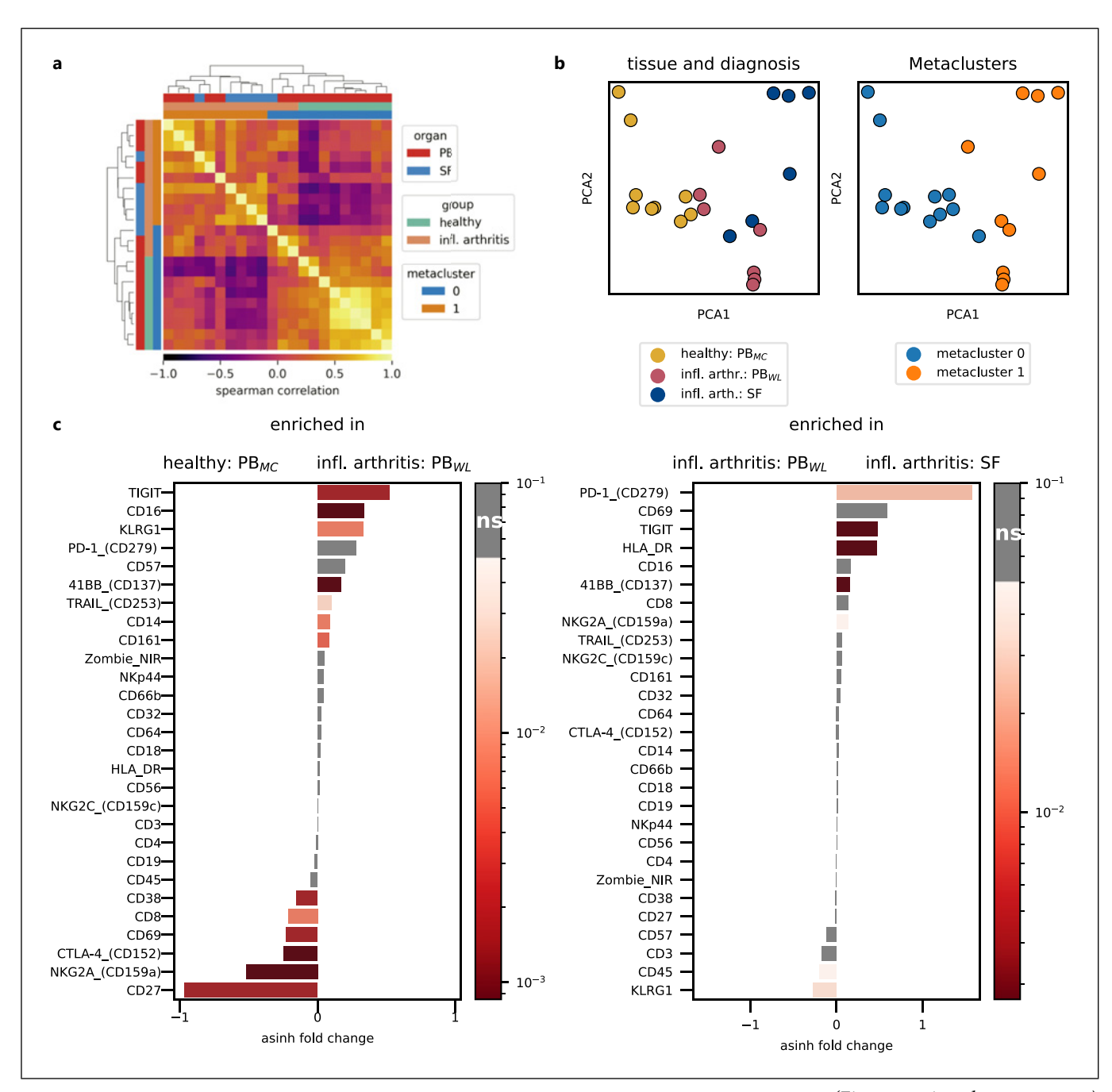


(Figure continued on next page.)

remained uncertain whether the SF-NK cell phenotype is rather influenced by inflammation-dependent activation or developmental stages. In order to better classify NK cell subsets, we calculated a differentiation rank score based on a composite measure of CD56, CD16, and CD57 [12, 40–43] on healthy NK cells that allowed us to have a more unbiased and continuous measure of NK cell mat-

uration. This approach is further backed by recent single-cell RNA-seq data that proposed the presence of three distinct NK cell subgroups, distinguished, among others, by the expression of CD56, CD16, and CD57 [44]. Our approach confirms that a difference in maturation states contributes to the differences between healthy and diseased blood and between PB and SF, with enriched immature NK

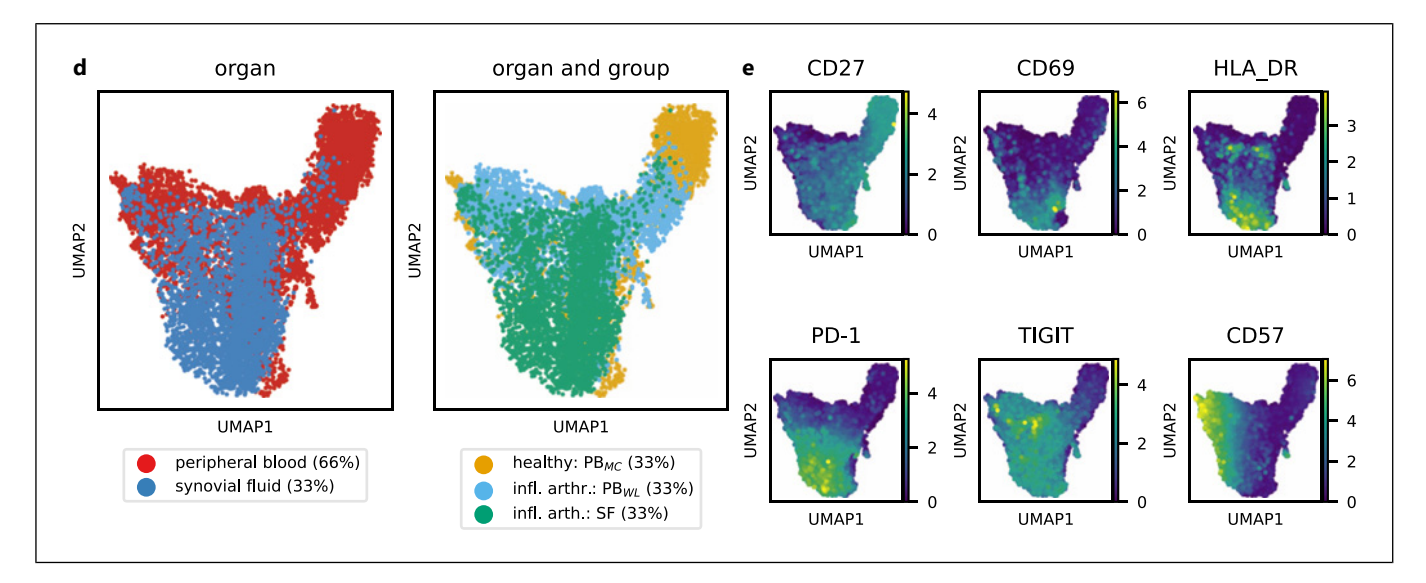


Fig. 4. Phenotypic heterogeneities of cytotoxic T lymphocytes in PB and SF of patients with IA. **a** Sample correlation analysis. Samples were correlated as described in the online supplementary Methods section. Hierarchical clustering revealed three subgroups which correspond to cells of different tissue and patient cohort. **b** Sample-wise PCA. Samples were grouped by PCA and coloured by tissue and patient cohort (left) and the metaclusters (right) as calculated in C. **c** Differential expression analysis. Fold-changes (*x*-axis, asinh_fc) were calculated as described in the online supplementary Methods section. Notably, CD8+T-cells analysed from PB show significant phenotypic differences comparing healthy controls and patients with IA, including expression changes of TIGIT, CD16, and CD27. Comparison of cells extracted from PB and SF show a differential phenotype with the elevation of activation markers

such as PD-1, CD69, and HLA-DR and the corresponding downregulation of CD27 and CD57. For comparison, the data are presented as boxplots in online supplementary Figure S6. $\bf d$ UMAP representation of cytotoxic T lymphocytes. Colouring by tissue and patient cohort suggests substantial differences of cells obtained from the different conditions. $\bf e$ Marker expression showed that SF-CD8+T-cells were characterized by lower expression of CD27 while elevating activation markers such as PD-1, HLA-DR, TIGIT, and CD69. p values were calculated as described in the Methods section (Kruskal) where p values above 0.05 were considered not significant (n.s.). Corresponding boxplot representations are shown in online supplementary Figure S6. Healthy controls (n = 9), IA patients (n = 7). PB, peripheral blood; SF, synovial fluid; IA, inflammatory arthritis.

cells in SF and depleted immature NK cells in patient blood. Furthermore, the absence of the CD57^{bright} population in the PB of arthritis patients indicates that the full maturation spectrum and ageing of NK cells is impaired in IA patients. This could be caused by the consumption of earlier NK cells at the site of inflammation, although we cannot rule out that changes in the cytokine signature or the general state of inflammation reduces NK cell maturation, in line with previous results [41]. Our results therefore suggest that maturation together with local activating stimuli drive the heterogeneity of SF-NK cells as indicated by metacluster analysis.

Elevated CTLA4, NKG2A, and CD69 Characterize SF-NK Cells and Indicate a Complex Immune Regulation

SF-NK cells exhibited complex phenotypes partly characterized by the up-regulation of immune checkpoints, especially NKG2A. NKG2A acts as an

inhibitory receptor and has been shown to limit excessive activation and cytokine production as well as promoting NK cell expansion [45, 46]. Here, NKG2A was found to be mostly expressed on immature, CD56^{bright} NK cells in line with previous studies [47, 48]. At the same time, NK cells from SF showed a significantly higher expression of CTLA4 compared to patient blood. CTLA4 functions as an inhibitory receptor on NK cells, similar to its role on T-cells [49-51]. Whether elevated CTLA4 on SF-NK cells modulates the therapeutic effect of abatacept, a CTLA4-Ig fusion protein used to treat RA, needs to be addressed in future studies. In addition to CD69, a marker for NK cell proliferation and cytotoxic activity [12, 52], we found further activation markers on SF-NK cells (HLA-DR, 41BB), suggesting that both differences in maturation and local cell activation concurrently drive NK cell phenotypes in inflamed SF.

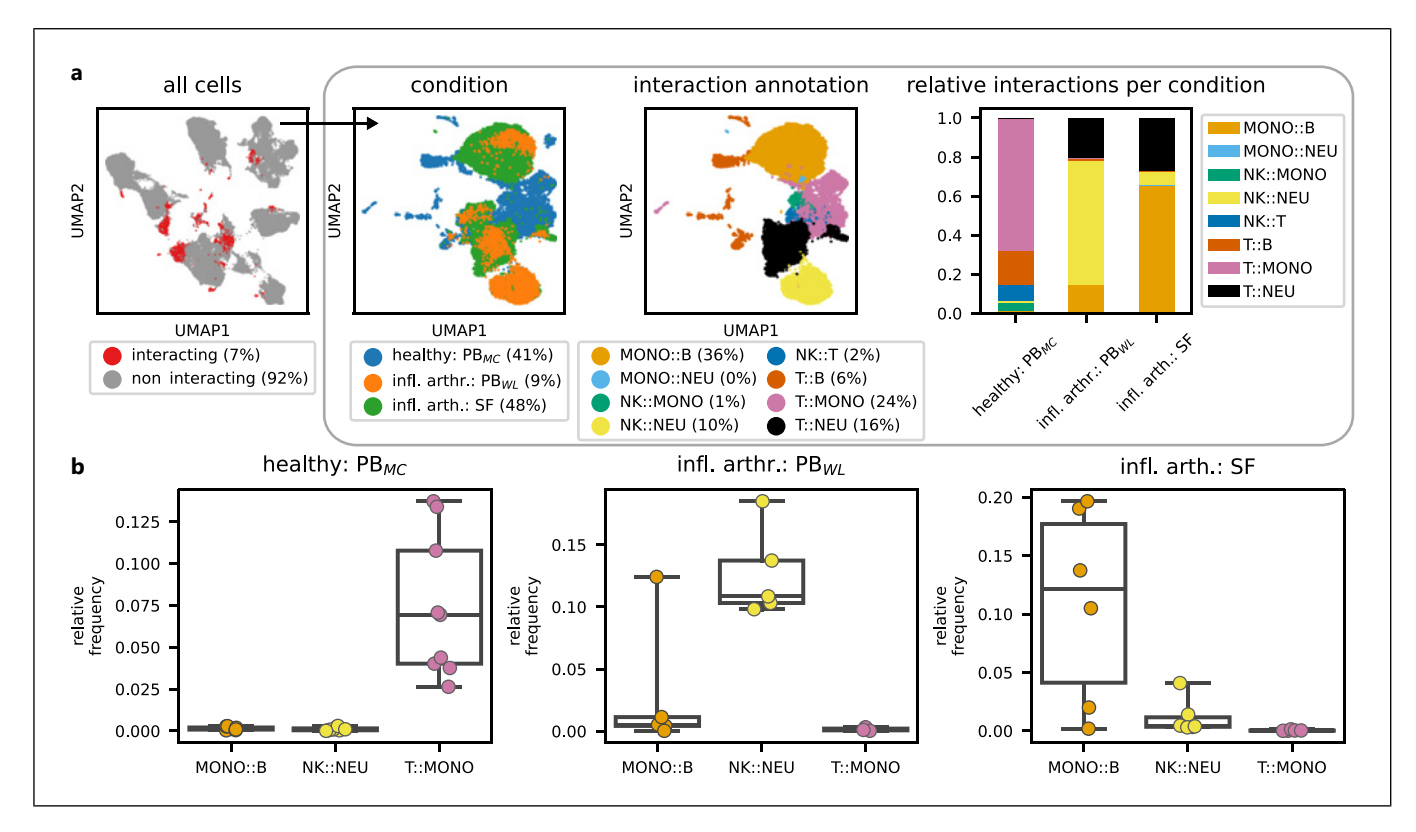


Fig. 5. Interact-omics across cell types in inflamed arthritis. **a** Interacting cells were selected by cluster annotation (left UMAP), reclustered (middle UMAP), and re-annotated (right UMAP). The stacked bar chart (right) shows the percentage of cell-cell interactions for each condition: healthy PB, inflamed arthritis SF, and inflamed arthritis PB. Samples to the left of the

black bar consisted of purified PBMC, while samples to the right were purified whole leukocytes. **b** Boxplots illustrating the fraction of selected interactions in each tissue. Each dot represents an individual sample. Healthy controls (n = 9), IA patients (n = 7). PB, peripheral blood; SF, synovial fluid; IA, inflammatory arthritis.

Cellular Interaction Landscape Reveals Mainly NK Cell/Neutrophil Interactions in Patients

As NK cells are clearly influenced by surrounding cells, we intended to identify neighbour cells that undergo tight binding as a surrogate of direct cell-cell interactions. Hypothesizing that tight intercellular binding is not disrupted during the applied conservation procedures, we leveraged a novel approach that allows cellular interaction mapping [13]. Using this approach, we were able to detect cell-cell interactions between T-cells and monocytes in healthy PB, while diseased patients were enriched for NK cell/neutrophil interactions and interactions between monocytes and B-cells, respectively. While slightly different cell isolation procedures preclude a direct comparison between patients and healthy controls in this study, it is still noteworthy that we were able to detect cell-cell interactions between T-cells and monocytes in healthy PB. The pathophysiologic relevance of cell-cell interactions between NK cells and neutrophils and the potential difference in cellular interactions between specific diseases and controls needs to be substantiated in future studies and in functional experiments.

Taken together, our paired analysis of lymphocyte surface proteomes showed profound differences between PB and SF. In SF, maturation stages and activation contribute to complex and heterogeneous NK cell subsets which are also characterized by enhanced checkpoint molecules like CTLA4 and NKG2A. While previous work indicated existence of immature synovial NK cells based on individual surface markers, we confirm this finding using more detailed phenotypic descriptions and differentiation rank mapping. This study further provides novel insights by implementing the interact-omics framework elucidating crosstalk of NK cells with other immune cells in blood and SF from patients. The extent to which NK cell/neutrophil interactions contribute to the pathophysiology of arthritis

and their potential as therapeutic targets need to be addressed in future investigations. Modulation of this crosstalk, either by immune-checkpoint-blockade or by disrupting critical mediators of pathogenic NK cell/neutrophil interaction holds promise to ameliorate joint inflammation without broadly compromising innate immune function.

Statement of Ethics

Written informed consent was obtained from all donors of PB and SF. Clinical data were gathered from patient records, and the local institutional review board approved this study (University of Heidelberg, S-272/2021). We received written informed consent from the individuals for the publication of personal metadata in a pseudonymized manner.

Conflict of Interest Statement

There are no direct competing interests regarding this manuscript. Senior physicians involved in this study, however, are involved in multiple interactions with (pharma/biotech) companies, in most cases of low financial relevance (e.g., consulting fees, honoraria for lectures/presentations, support for attending meetings and/or travel, research funding). Find individual statements from all authors below. F.S.D., T.E., M.C., S.Y., L.R., C.W., S.H., D.H., and S.E.L.: there are no conflicts of interest regarding this project. J.H.W.D. has received grants or contracts from: AbbVie, Anamar, Argenx, ARXX, BMS, Bayer Pharma, Boehringer-Ingelheim, Cantargia, Celgene, CSL Behring, ExoTherapeutics, Galapagos, GSK, Inventiva, Kiniksa, Lassen, Novartis, Sanofi-Aventis, RedX and UCB; consulting fees from: AbbVie, Active Biotech, Anamar, ARXX, AstraZeneca, Bayer Pharma, Boehringer-Ingelheim, Celgene, Galapagos, Genentech, GSK, Inventiva, Janssen, Novartis, Pfizer, Roche and UCB; payment or honoraria for lectures, presentations, speakers bureaus, manuscript writing or educational events from: AbbVie, Active Biotech, Anamar, ARXX, AstraZeneca, Bayer Pharma, Boehringer-Ingelheim, Celgene, Galapagos, Genentech, GSK, Inventiva, Janssen, Novartis, Pfizer, Roche and UCB; Payment for expert testimony from: AbbVie, Anamar, ARXX, AstraZeneca, Bayer Pharma, Boehringer-Ingelheim, Cantargia, Celgene, Galapagos, Genentech, GSK, Inventiva, Janssen, Novartis, Pfizer, Roche and UCB; support for attending meetings and/or travel from: AbbVie, SOBI; Stock or stock options from: 4D Science; FibroCure; receipt of equipment, materials, drugs, medical writing, gifts, or other services from: Boehringer-Ingelheim. H.-M.L. has received grants from Abbvie, AstraZeneca, Actelion, Alexion, Amgen, Bayer Vital, Baxter, Biocon, Biogen, Boehringer-Ingelheim, BMS, Celgene, Celltrion, Chugai, Fresenius, Galapagos, Genzyme, GSK, Gilead, Hexal, Janssen-Cilag, Lilly, Medac, MSD, Mundipharm, Mylan, Nordic, Novartis, octapharm, Pfizer, Roche, Sandoz, Sanofi, Shire, SOBI, Stada, Takeda, Thermo Fisher, UCB, Vifor; consulting fees from: Abbvie, AstraZeneca, Boehringer-Ingelheim, Galapagos, GSK, Novartis, Pfizer, Roche; Payment or honoraria for lectures, presentations, speakers bureaus, manuscript writing or educational events from: Abbvie, AstraZeneca, Actelion, Alexion, Amgen, Bayer Vital, Baxter, Biocon, Biogen, Boehringer-Ingelheim, BMS, Celgene, Celltrion, Chugai, Fresenius, Galapagos, Genzyme, GSK, Gilead, Hexal, Janssen-Cilag, Lilly, Medac, MSD, Mundipharm, Mylan, Nordic, Novartis, octapharm, Pfizer, Roche, Sandoz, Sanofi, Shire, SOBI, Stada, Takeda, Thermo Fisher, UCB, Vifor. Support for attending meetings and/ or travel from Abbvie, AstraZeneca, Boehringer-Ingelheim, BMS, Chugai, Galapagos, GSK, Janssen-Cilag, Lilly, Medac, MSD, Novartis, Pfizer, Roche, UCB; Participation on a Data Safety Monitoring Board or Advisory Board from: Abbvie, AstraZeneca, Boehringer-Ingelheim, Galapagos, GSK, Novartis, Pfizer, Roche. W.M. has received grants or contracts from German Society of Internal Medicine (DGIM), ArgenX, Kyverna, Lilly, Galapagos, Boehringer-Ingelheim, Evotec, BMS; consulting fees and payment or honoraria for lectures and presentations from Lilly, Galapagos, Boehringer-Ingelheim; support for attending meetings and/or travel Kyverna, Lilly, Galapagos, Boehringer-Ingelheim; patents planned Evotec, BMS; Participation on an Advisory Board: Lilly, Boehringer-Ingelheim; receipt of equipment, materials, drugs: ArgenX.

Funding Sources

T.E. was partially funded by the structured doctoral programme (*Strukturiertes Doktorandenprogramm zum Erwerb des Dr. med. und Dr. rer. nat.*) of Heidelberg University. The authors acknowledge support by the state of Baden-Württemberg through bwHPC and the German Research Foundation (DFG) through grant INST 35/1597-1 FUGG. W.M. was funded by the Advanced Clinician Scientist programme of the DGIM. All other authors declare no further funding sources.

Author Contributions

Conceptualization: F.S.D. and W.M., Methodology: F.S.D, M.C., T.E., and S.Y., Software: T.E. and S.Y., Validation and resources: N/A. Formal analysis: F.S.D., T.E., M.C., L.R., S.E.L, and S.Y., Investigation: F.S.D., T.E., M.C., L.R., S.E.L, S.Y., and S.H., Data curation: F.S.D., M.C., L.R., and S.E.L., Writing – original draft: F.S.D., T.E., and W.M., Writing – editing: F.S.D., T.E., M.C., L.R., S.E.L., W.M., S.H., and S.Y., Visualization: F.S.D. and T.E., Supervision: W.M., C.W., and D.H., Project administration: W.M., C.W., D.H., J.H.W.D., and H.-M.L., Funding acquisition: W.M., H.-M.L., and C.W.

Data Availability Statement

Flow cytometry data are available upon request. The data that support the findings of this study are not publicly available due to privacy reasons but are available from the corresponding author upon request. The code to reproduce the analysis and to generate the figures was publicly deposited under https://github.com/TarikExner/NK_cell_compartments_paper.

References

- 1 Merkt W, Salzer U, Thiel J, Jandova I, Bergner R, Venhoff AC, et al. Blood CD3-(CD56 or 16)+ natural killer cell distributions are heterogeneous in healthy adults and suppressed by azathioprine in patients with ANCA-associated vasculitides. BMC Immunol. 2021;22(1):26. https://doi.org/10.1186/s12865-021-00416-w
- 2 Vivier E, Tomasello E, Baratin M, Walzer T, Ugolini S. Functions of natural killer cells. Nat Immunol. 2008;9(5):503–10. https://doi. org/10.1038/ni1582
- 3 Caligiuri MA. Human natural killer cells. Blood. 2008;112(3):461–9. https://doi.org/ 10.1182/blood-2007-09-077438
- 4 Cooper MA, Fehniger TA, Caligiuri MA. The biology of human natural killer-cell subsets. Trends Immunol. 2001;22(11):633–40. https://doi.org/10.1016/s1471-4906(01) 02060-9
- 5 Firestein GS, McInnes IB. Immunopathogenesis of rheumatoid arthritis. Immunity. 2017;46(2):183–96. https://doi.org/10.1016/j.immuni.2017.02.006
- 6 Dalbeth N, Callan MF. A subset of natural killer cells is greatly expanded within inflamed joints. Arthritis Rheum. 2002;46(7): 1763–72. https://doi.org/10.1002/art.10410
- 7 Yamin R, Berhani O, Peleg H, Aamar S, Stein N, Gamliel M, et al. High percentages and activity of synovial fluid NK cells present in patients with advanced stage active rheumatoid arthritis. Sci Rep. 2019;9(1):1351. https://doi.org/10.1038/s41598-018-37448-z
- 8 Zhao S, Grieshaber-Bouyer R, Rao DA, Kolb P, Chen H, Andreeva I, et al. Effect of JAK inhibition on the induction of proinflammatory HLA-DR+CD90+ rheumatoid arthritis synovial fibroblasts by Interferon-γ. Arthritis Rheumatol. 2022;74(3):441–52. https://doi.org/10.1002/art.41958
- 9 Carmona-Rivera C, Carlucci PM, Moore E, Lingampalli N, Uchtenhagen H, James E, et al. Synovial fibroblast-neutrophil interactions promote pathogenic adaptive immunity in rheumatoid arthritis. Sci Immunol. 2017;2(10):eaag3358. https://doi.org/ 10.1126/sciimmunol.aag3358
- 10 Pridgeon C, Lennon GP, Pazmany L, Thompson RN, Christmas SE, Moots RJ. Natural killer cells in the synovial fluid of rheumatoid arthritis patients exhibit a CD56bright,CD94bright,CD158negative phenotype. Rheumatology. 2003;42(7): 870-8. https://doi.org/10.1093/rheumatology/keg240
- 11 McQueen FM, Dalbeth N. Predicting joint damage in rheumatoid arthritis using MRI scanning. Arthritis Res Ther. 2009;11(5):124. https://doi.org/10.1186/ar2778
- 12 Attrill MH, Shinko D, Alexiou V, Kartawinata M; CHARMS study; JIAP study, et al. The immune landscape of the inflamed joint defined by spectral flow cytometry. Clin Exp

- Immunol. 2024;218(3):221-41. https://doi.org/10.1093/cei/uxae071
- 13 Vonficht D, Jopp-Saile L, Yousefian S, Flore V, Simó Vesperinas I, Teuber R, et al. Ultrahigh-scale cytometry-based cellular interaction mapping. Nat Methods. 2025;22(9): 1887–99. https://doi.org/10.1038/s41592-025-02744-w
- 14 Virshup I, Rybakov S, Theis FJ, Angerer P, Wolf FA. Anndata: access and Store annotated data matrices. J Open Source Softw. 2024;9(101):4371. https://doi.org/10.21105/joss.04371
- Traag VA, Waltman L, van Eck NJ. From louvain to leiden: guaranteeing well-connected communities. Sci Rep. 2019/03/26 2019;9(1):5233. https://doi.org/10.1038/s41598-019-41695-z
- 16 McInnes L, Healy J, Saul N, Großberger L. UMAP: uniform manifold approximation and projection. J Open Source Softw. 2018; 3(29):861. https://doi.org/10.21105/joss. 00861
- 17 Virshup I, Bredikhin D, Heumos L, Palla G, Sturm G, Gayoso A, et al. The scverse project provides a computational ecosystem for single-cell omics data analysis. Nat Biotechnol. 2023;41(5):604–6. https://doi.org/10.1038/s41587-023-01733-8
- 18 Coifman RR, Lafon S, Lee AB, Maggioni M, Nadler B, Warner F, et al. Geometric diffusions as a tool for harmonic analysis and structure definition of data: diffusion maps. Proc Natl Acad Sci U S A. 2005;102(21): 7426–31. https://doi.org/10.1073/pnas. 0500334102
- 19 Haghverdi L, Buettner F, Theis FJ. Diffusion maps for high-dimensional single-cell analysis of differentiation data. Bioinformatics. 2015;31(18):2989–98. https://doi.org/10. 1093/bioinformatics/btv325
- 20 Emmaneel A, Quintelier K, Sichien D, Rybakowska P, Marañón C, Alarcón-Riquelme ME, et al. PeacoQC: peak-Based selection of high quality cytometry data. Cytometry A. 2022;101(4):325–38. https://doi.org/10.1002/cyto.a.24501
- 21 Hao Y, Stuart T, Kowalski MH, Choudhary S, Hoffman P, Hartman A, et al. Dictionary learning for integrative, multimodal and scalable single-cell analysis. Nat Biotechnol. 2024;42(2):293–304. https://doi.org/10.1038/s41587-023-01767-y
- 22 Blondel VD, Guillaume J-L, Lambiotte R, Lefebvre E. Fast unfolding of communities in large networks. J Stat Mech. 2008 2008; 2008(10):10008. https://doi.org/10.1088/ 1742-5468/2008/10/p10008
- 23 Astorga-Gamaza A, Perea D, Sanchez-Gaona N, Calvet-Mirabent M, Gallego-Cortés A, Grau-Expósito J, et al. KLRG1 expression on natural killer cells is associated with HIV persistence, and its targeting promotes the reduction of the viral reservoir. Cell Rep

- Med. 2023;4(10):101202. https://doi.org/10.1016/j.xcrm.2023.101202
- 24 Yang ZZ, Kim HJ, Wu H, Jalali S, Tang X, Krull JE, et al. TIGIT expression is associated with T-cell suppression and exhaustion and predicts clinical outcome and Anti-PD-1 response in follicular lymphoma. Clin Cancer Res. 2020;26(19):5217–31. https://doi.org/10.1158/1078-0432.Ccr-20-0558
- 25 Zumwalde NA, Domae E, Mescher MF, Shimizu Y. ICAM-1-dependent homotypic aggregates regulate CD8 T cell effector function and differentiation during T cell activation. J Immunol. 2013;191(7): 3681-93. https://doi.org/10.4049/jimmunol.1201954
- 26 Pauken KE, Shahid O, Lagattuta KA, Mahuron KM, Luber JM, Lowe MM, et al. Single-cell analyses identify circulating antitumor CD8 T cells and markers for their enrichment. J Exp Med. 2021;218(4): e20200920. https://doi.org/10.1084/jem. 20200920
- 27 Georg P, Astaburuaga-García R, Bonaguro L, Brumhard S, Michalick L, Lippert LJ, et al. Complement activation induces excessive T cell cytotoxicity in severe COVID-19. Cell. 2022;185(3):493–512.e25. https://doi.org/10. 1016/j.cell.2021.12.040
- 28 Klocperk A, Friedmann D, Schlaak AE, Unger S, Parackova Z, Goldacker S, et al. Distinct CD8 T cell populations with differential exhaustion profiles associate with secondary complications in common variable immunodeficiency. J Clin Immunol. 2022;42(6):1254–69. https://doi.org/10.1007/s10875-022-01291-9
- 29 Ebihara T, Yamada T, Fuchimukai A, Takasuga S, Endo T, Yamada T, et al. Dysfunction of type 1 and type 2 immune cells: a lesson from exhausted-like ILC2s and their activation-induced cell death. Int Immunol. 2024;36(11):585–94. https://doi.org/10.1093/ intimm/dxae032
- 30 Straube J, Bukhari S, Lerrer S, Winchester RJ, Gartshteyn Y, Henick BS, et al. PD-1 signaling uncovers a pathogenic subset of T cells in inflammatory arthritis. Arthritis Res Ther. 2024;26(1):32. https://doi.org/10.1186/s13075-023-03259-5
- 31 Vanni A, Mazzoni A, Semeraro R, Capone M, Maschmeyer P, Lamacchia G, et al. Clonally expanded PD-1-expressing T cells are enriched in synovial fluid of juvenile idiopathic arthritis patients. Eur J Immunol. 2023;53(7):e2250162. https://doi.org/10.1002/eji.202250162
- 32 Anaparti V, Tanner S, Zhang C, O'Neil L, Smolik I, Meng X, et al. Increased frequency of TIGIT+ CD4 T Cell subset in autoantibody-positive first-degree relatives of patients with rheumatoid arthritis. Front Immunol. 2022;13:932627. https://doi.org/10.3389/fimmu.2022.932627

- 33 Chauvin JM, Pagliano O, Fourcade J, Sun Z, Wang H, Sander C, et al. TIGIT and PD-1 impair tumor antigen-specific CD8+ T cells in melanoma patients. J Clin Investig. 2015; 125(5):2046-58. https://doi.org/10.1172/jci80445
- 34 van Bijnen ST, Cossu M, Roeven MWH, Jansen TL, Preijers F, Spanholtz J, et al. Functionally active NKG2A-expressing natural killer cells are elevated in rheumatoid arthritis patients compared to psoriatic arthritis patients and healthy donors. Clin Exp Rheumatol. 2015;33(6):795–804.
- 35 Dalbeth N, Gundle R, Davies RJ, Lee YC, McMichael AJ, Callan MF. CD56bright NK cells are enriched at inflammatory sites and can engage with monocytes in a reciprocal program of activation. J Immunol. 2004; 173(10):6418–26. https://doi.org/10.4049/jimmunol.173.10.6418
- 36 Shibatomi K, Ida H, Yamasaki S, Nakashima T, Origuchi T, Kawakami A, et al. A novel role for interleukin-18 in human natural killer cell death: high serum levels and low natural killer cell numbers in patients with systemic autoimmune diseases. Arthritis Rheum. 2001;44(4):884–92. https://doi.org/10.1002/1529-0131(200104)44:4<884::aid-anr145>3.3.co;2-w
- 37 Kurioka A, Cosgrove C, Simoni Y, van Wilgenburg B, Geremia A, Björkander S, et al. CD161 defines a functionally distinct subset of pro-inflammatory natural killer cells. Front Immunol. 2018;9:486. https://doi.org/10.3389/fimmu.2018.00486
- 38 Abel AM, Yang C, Thakar MS, Malarkannan S. Natural killer cells: development, maturation, and clinical utilization. Front Immunol. 2018;9:1869. https://doi.org/10.3389/ fimmu.2018.01869
- 39 de Matos CT, Berg L, Michaëlsson J, Felländer-Tsai L, Kärre K, Söderström K. Activating and inhibitory receptors on synovial fluid natural

- killer cells of arthritis patients: role of CD94/ NKG2A in control of cytokine secretion. Immunology. 2007;122(2):291–301. https://doi.org/10.1111/j.1365-2567.2007.02638.x
- 40 Lopez-Vergès S, Milush JM, Pandey S, York VA, Arakawa-Hoyt J, Pircher H, et al. CD57 defines a functionally distinct population of mature NK cells in the human CD56dimCD16+ NK-cell subset. Blood. 2010;116(19):3865–74. (in eng).https://doi.org/10.1182/blood-2010-04-282301
- 41 Nielsen CM, White MJ, Goodier MR, Riley EM. Functional significance of CD57 expression on human NK cells and relevance to disease. Front Immunol. 2013;4:422. https://doi.org/10.3389/fimmu.2013.00422
- 42 Crinier A, Dumas PY, Escalière B, Piperoglou C, Gil L, Villacreces A, et al. Single-cell profiling reveals the trajectories of natural killer cell differentiation in bone marrow and a stress signature induced by acute myeloid leukemia. Cell Mol Immunol. 2021;18(5): 1290–304. https://doi.org/10.1038/s41423-020-00574-8
- 43 Yang C, Siebert JR, Burns R, Gerbec ZJ, Bonacci B, Rymaszewski A, et al. Heterogeneity of human bone marrow and blood natural killer cells defined by single-cell transcriptome. Nat Commun. 2019;10(1): 3931. https://doi.org/10.1038/s41467-019-11947-7
- 44 Rebuffet L, Melsen JE, Escalière B, Basurto-Lozada D, Bhandoola A, Björkström NK, et al. High-dimensional single-cell analysis of human natural killer cell heterogeneity. Nat Immunol. 2024;25(8):1474–88. https://doi.org/10.1038/s41590-024-01883-0
- 45 Borrego F, Kabat J, Sanni TB, Coligan JE. NK cell CD94/NKG2A inhibitory receptors are internalized and recycle independently of inhibitory signaling processes. J Immunol. 2002;169(11):6102–11. https://doi.org/10.4049/jimmunol.169.11.6102

- 46 Kamiya T, Seow SV, Wong D, Robinson M, Campana D. Blocking expression of inhibitory receptor NKG2A overcomes tumor resistance to NK cells. J Clin Investig. 2019; 129(5):2094–106. https://doi.org/10.1172/ jci123955
- 47 Wang X, Xiong H, Ning Z. Implications of NKG2A in immunity and immunemediated diseases. Front Immunol. 2022; 13:960852. https://doi.org/10.3389/fimmu. 2022.960852
- 48 Béziat V, Descours B, Parizot C, Debré P, Vieillard V. NK cell terminal differentiation: correlated stepwise decrease of NKG2A and acquisition of KIRs. PLoS One. 2010;5(8): e11966. https://doi.org/10.1371/journal.pone.0011966
- 49 Stojanovic A, Fiegler N, Brunner-Weinzierl M, Cerwenka A. CTLA-4 is expressed by activated mouse NK cells and inhibits NK Cell IFN-γ production in response to mature dendritic cells. J Immunol. 2014;192(9): 4184–91. https://doi.org/10.4049/jimmunol. 1302091
- 50 Davis-Marcisak EF, Fitzgerald AA, Kessler MD, Danilova L, Jaffee EM, Zaidi N, et al. Transfer learning between preclinical models and human tumors identifies conserved NK cell activation signature in anti-CTLA-4 responsive tumors. bioRxiv. 2021:2020. https://doi.org/10.1101/2020.05.31.125625
- 51 Hossen MM, Ma Y, Yin Z, Xia Y, Du J, Huang JY, et al. Current understanding of CTLA-4: from mechanism to autoimmune diseases. Front Immunol. 2023;14:1198365. https://doi.org/10.3389/fimmu.2023. 1198365
- 52 Borrego F, Robertson MJ, Ritz J, Peña J, Solana R. CD69 is a stimulatory receptor for natural killer cell and its cytotoxic effect is blocked by CD94 inhibitory receptor. Immunology. 1999;97(1):159–65. https://doi.org/10.1046/j.1365-2567.1999.00738.x